Journal of Alloys and Compounds 509 (2011) 5200–5205

Contents lists available at ScienceDirect

Journal of Alloys and Compounds

journal homepage: www.elsevier.com/locate/jallcom

Crystal structure and magnetic properties of V-doped YCo_2 and YCo_3 and their hydrides

H. Michor[a,*], G. Hilscher[a], O. Myakush[b], N. Pyk[b], P. Myronenko[b], I. Koval'chuck[c], B. Kotur[b]

[a] *Institute of Solid State Physics, Vienna University of Technology, Wiedner Hauptstrasse 8-10, A-1040 Vienna, Austria*
[b] *Department of Inorganic Chemistry, Ivan Franko National University of Lviv, Kyryla and Mefodia Str. 6, UA-79005 Lviv, Ukraine*
[c] *H.V. Karpenko Physico-Mechanical Institute, National Academy of Science of Ukraine, Naukova Str. 5, UA-79601 Lviv, Ukraine*

ARTICLE INFO

Article history:
Received 22 December 2010
Received in revised form 7 February 2011
Accepted 8 February 2011
Available online 15 February 2011

Keywords:
Yttrium intermetallic compound
Crystal structure
Hydride
Magnetic properties

ABSTRACT

Pseudo-binary $YCo_{3-x}V_x$ and $YCo_{2-x}V_x$ ($x = 0.1$ and 0.2) phases have been investigated for the influence of V-doping on the crystal structure and magnetic properties of YCo_3 ($PuNi_3$-type, space group $R\bar{3}m$) and YCo_2 ($MgCu_2$-type, space group $Fd\bar{3}m$) and their hydrides. All substituted solid solutions preserve the structure of the binary parent compounds. The lattice parameters increase with increasing V content. All investigated compounds and solid solutions can easily absorb hydrogen up to 3.2–3.9 at.H/f.u. at room temperature at 0.1–0.12 MPa pressure without amorphization. YCo_3 and solid solutions $YCo_{3-x}V_x$ show ferrimagnetic behaviour where Co/V substitution reduces T_c from 301 K of YCo_3 to 225 K in $YCo_{2.8}V_{0.2}$. Hydrogenation causes complex antiferromagnetism below 200 K in the γ-phase hydrides with a reduced mean 3d-moment at low temperatures. Substitution of Co by V induces weak ferromagnetism in the archetypical itinerant electron metamagnet YCo_2 with Curie temperatures of 175 K and 110 K and a mean 3d-moment of $0.14\mu_B$ and $0.07\mu_B$ at 6 T and 2.5 K for $x = 0.1$ and $x = 0.2$, respectively. Hydrogen absorption enhances the mean 3d-moment slightly but reduces the ordering temperature to below 30 K in the corresponding β-phase hydrides. A ferromagnetic background occurs in all YCo_2 and YCo_3 based hydrides persisting up to above room temperature which is of different origin but appears to be not an intrinsic property of these hydrides.

1. Introduction

Various metals and alloys absorb large quantities of hydrogen. Among them are intermetallics RCo_n (R = rare earth, $n = 2$ or 3) which have been studied in more detail in the past when searching for promising electrochemical energy storage materials [1,2].

Binary RCo_3 (except Pm and Eu) compounds crystallize in the rhombohedral $PuNi_3$-type (space group $R\bar{3}m$) [3]. The $PuNi_3$ contains $CaCu_5$ (Haucke phase) and $MgZn_2$ (Laves phase) structure fragments [4] and can conveniently be described in terms of an alternate stacking of RCo_5 and RCo_2 blocks along the *c*-axis with a ratio 1:2. Apart from the rich variety of magnetic properties of RCo_3 compounds with 3 different Co sites, there exists from both the theoretical and experimental point of view a controversial debate whether the ground state of YCo_3 is ferro- or ferrimagnetic (see e.g. [5] and references therein). Combining neutron powder diffraction and density functional theory band structure calculations Cui et al. [5] conclude that the ferrimagnetic ground state is the stable one, where the moments at Co2 sites are antiparallel to the two other Co sites, although a ferromagnetic state can be achieved also in terms of fixed spin moment calculations in high fields. This is in line with various earlier reports where the ferrimagnetic ground state denoted earlier as the weak itinerant ferromagnetic state (with $0.5\mu_B$/Co) can be transformed into a saturated ferromagnetic (with $1.2\mu_B$/Co) ground state via two field induced metamagnetic transitions in ultra high fields [6,7].

RCo_3 compounds exhibit interesting hydrogen storage properties under ambient temperature and pressure conditions, for reviews see Refs. [1,2,8]. Absorption of hydrogen causes a significant volume expansion and leads to formation of the two stable hydrides, the β- and γ-phase. In particular the itinerant-electron ferrimagnet YCo_3 forms a stable β-phase YCo_3H_x ($1 \le x \le 1.9$) at about 0.005 atm [9–11], which actually was found to contain two phases, the β_1 ($1 < x < 1.5$) and β_2 phase ($1.5 < x < 2$) [12], and the γ-phase YCo_3H_x ($3.4 \le x \le 4.0$) at about 0.45 atm hydrogen pressure [11,13]. There are a number of reports on the magnetic properties of both β and γ hydride phases [6–15]. Using ultra high magnetic fields up to 130 T and band structure calculations lead to a deeper understanding of the complex magnetic properties due to a hydrogen induced modification of the density of states (DOS) and the associated Co moments at different lattice sites. The β_1 hydrides exhibit pronounced metamagnetic transitions at about

---

* Corresponding author. Tel.: +43 1 58801 13140; fax: +43 1 58801 13199.
E-mail address: michor@ifp.tuwien.ac.at (H. Michor).

0925-8388/$ – see front matter © 2011 Elsevier B.V. All rights reserved.
doi:10.1016/j.jallcom.2011.02.052

Table 1
Crystallographic parameters of the $YCo_{3-x}V_x$ ($x = 0$, 0.1 and 0.2) alloys and their hydrides ($PuNi_3$-type, space group $R\bar{3}m$).

Alloys and hydrides	a(Å)	c(Å)	c/a	V(Å^3)	$\Delta V/V$ (%)	H/M
YCo_3	5.01442(1)	24.3572(1)	4.857	530.39(1)		
$YCo_3H_{3.90}$	5.2453(1)	26.674(1)	5.085	635.58(1)	19.83	0.98
$YCo_{2.9}V_{0.1}$	5.01800(1)	24.3339(1)	4.849	530.64(1)		
$YCo_{2.9}V_{0.1}H_{3.67}$	5.2454(4)	26.392(3)	5.031	628.87(3)	18.51	0.92
$YCo_{2.8}V_{0.2}$	5.0241(3)	24.317(2)	4.840	531.65(2)		
$YCo_{2.8}V_{0.2}H_{3.75}$	5.2640 (7)	26.449(4)	5.024	634.71(3)	19.38	0.94

$\Delta V/V^* = [V(\text{hydride}) - V(\text{parent alloy})]/V(\text{parent alloy}) \times 100\%$; where V—unit cell volume; H/M^{**}—ratio of H atoms per metal atoms in the hydride.

20 T accompanied by a large hysteresis and the β_2 phase shows a further metamagnetic transition at about 80 T. Their magnetic states where initially characterized as (i) weakly ferromagnetic (with a mean Co moment of about 0.1–0.2μ_B/Co), (ii) intermediately saturated ferromagnetic (0.4–0.8μ_B/Co) and (iii) saturated ferromagnetic (1.2μ_B/Co) [7]. Bartashevich et al. [6] succeeded to prepare a $YCo_3H_{3.9}$ single crystal of the γ-phase and observed a metamagnetic transition at about 18 T along the c-axis from the antiferromagnetic state into a forced ferromagnetic state. The ferromagnetic structure of the β_2-phase and the rather complex antiferromagnetic structure of the γ-phase could be resolved with synchrotron X-ray and neutron powder diffraction by Liu et al. [16]: Different Co moments occur on the three inequivalent Co-sites and the magnetic interactions between them are supposed to depend sensitively upon Co–Co distance, i.e. antiferromagnetic interactions occur for distances less than 2.44 Å and ferromagnetic coupling between 2.44 and 2.84 Å.

Various substitutions in one of the sublattices have been widely used to modify the hydrogenation properties of intermetallic compounds and particularly to adapt the plateau pressure of the hydrogenation process [1]. Substitutions of Co by Ni or Fe have been studied [8,15] without improving significantly the reversible hydrogen capacities of these alloys. The substitution of Co by Ga slightly decreases the hydrogen storage capacity [17].

RCo_2 cubic Laves phases have been of particular interest because they exhibit a large variety of magnetic phenomena which are reviewed in Refs. [18,19]. YCo_2 is the archetypical itinerant electron metamagnet showing a transition from a para- to a ferromagnetism at a critical field $B_c = 69$ T at 4.2 K [20]. YCo_2 can absorb hydrogen up to the composition of $YCo_2H_{3.5}$ and forms two crystalline hydrides: α-phase ($x \leq 0.3$) and the β-phase ($1.5 \leq x \leq 3.5$) [21]. The α-phase is an itinerant electron metamagnet whose critical field is possibly lower than that of the parent compound. The β-phase is a weak itinerant ferromagnet with a Co moment of 0.25μ_B at 45 T and 4.2 K and exhibits no metamagnetic transition [22]. Hydrogen absorption at higher temperatures associated with a violent reaction brings about significant structural disorder and eventually leads to an amorphous material which is a strong ferromagnet [22,23].

So far, several authors studied the influence of R by R′ (R and R′ are different species of rare earth elements) [24] and Co by Fe [24,25], Al [22], Ga [17], and Ti [26] substitutions and hydrogen-induced effects [20–25] on the crystal structure and magnetic properties of RCo_2 and related compounds. Recently we started to investigate the effect of Co by V and Co by Fe substitutions upon hydrogenation and magnetic properties of $ErCo_2$ [27]. Hydrogenation suppresses both the metamagnetic behaviour and long range magnetic order, i.e. reduces T_c.

This report focuses on the influence of partial substitutions of Co by V on the crystal structure and magnetic properties of the pseudo-binaries $YCo_{2-x}V_x$ and $YCo_{3-x}V_x$ and their hydrides.

2. Experimental procedure

Alloys have been prepared by arc melting of the initial elements with a purity not less than 99.9 wt.% under argon. During arc melting the weight losses were less than 1% of the total mass of the ingots. The alloys were annealed in quartz ampoules under vacuum at 600 °C for 720 h.

All hydrides were smoothly synthesized at room temperature under 0.1–0.12 MPa hydrogen pressure in an autoclave after preliminary activation of the samples in vacuum at 350–400° C, since it is known that hydrogenation at higher temperatures gives rise to amorphous YCo_2H_3 with a with a Curie temperature above 500 K [22,23]. The amount of absorbed hydrogen was determined by volumetric measurements.

The samples were examined by X-ray powder diffraction using diffractometers DRON-2.0 (FeK_α-radiation) and DRON-3M (Cu-K_α-radiation). For crystal structure determination the diffraction data were collected using a θ–2θ scan mode with steps of 0.05° 2θ and exposition times of 20 s at every point. All the crystal structure calculations were performed by the Rietveld method [28] using the FullProf [29] and CSD [30] programs.

Magnetization measurements have been performed in the temperature range 2–300 K in two different Cryogenic SQUID magnetometers with magnetic fields up to 6 T and 7 T, respectively.

3. Results and discussion

The XRD pattern of binary YCo_3 and substituted pseudo-binaries $YCo_{3-x}V_x$ ($x = 0.1$ and 0.2), see Fig. 1a are indexed in the rhombohedral $PuNi_3$-type structure (space group $R\bar{3}m$). The XRD pattern of $YCo_{2.8}V_{0.2}$ is presented in Fig. 1a. The profile refinement shows that the replacement of Co by V in YCo_3 does not change the structure type of the parent compound. The lattice parameters and cell volumes increase with increasing V content (Table 1). The refined final atomic parameters of $YCo_{3-x}V_x$ ($x = 0.2$) are presented in Table 2.

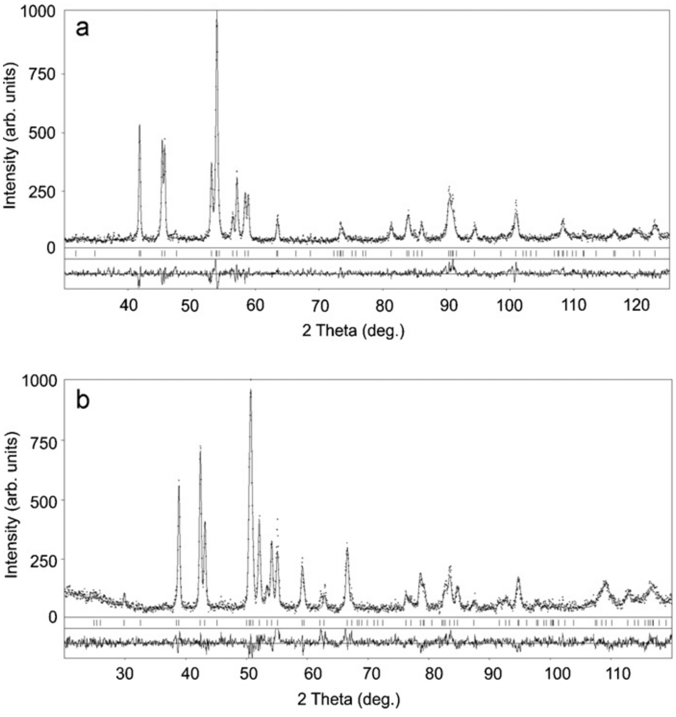

Fig. 1. Observed (points), calculated (line) and difference (bottom) X-ray diffraction patterns of $YCo_{2.8}V_{0.2}$ (a) and $YCo_{2.8}V_{0.2}H_{3.75}$ hydride (b).

Table 2
Refined atomic parameters, site occupations (G) and isotropic temperature coefficients (B_{iso}) for $YCo_{3-x}V_x$ ($x = 0.2$) ($PuNi_3$-type structure, $R_I = 0.0585$).

Atom	Site	x/a	y/b	z/c	G	B_{iso} (Å^2)
Y1	3*a*	0	0	0	1.0	0.95(2)
Y2	6*c*	0	0	0.1405(3)	1.0	0.70(1)
Co1	3*b*	0	0	0.5	1.0	0.71(1)
Co2	6*c*	0	0	0.3334(4)	0.69(1) Co + 0.31(1) V	0.79(1)
Co3	18*h*	0.8375(4)	0.1625(4)	0.5849(3)	1.0	0.72(1)

Table 3
Lattice parameters of the solid solution $YCo_{2-x}V_x$ and their hydrides ($MgCu_2$-type, space group $Fd\bar{3}m$).

Alloys and hydrides	a(Å)	V(Å^3)	$\Delta V/V$ (%)	H/M
YCo_2	7.2226(1)	376.77(1)		
$YCo_2H_{3.5}$	7.712(1)	458.67(1)	21.74	1.17
$YCo_{1.9}V_{0.1}$	7.2320(1)	378.25(1)		
$YCo_{1.9}V_{0.1}H_{3.2}$	7.686(3)	454.05(3)	20.04	1.07
$YCo_{1.8}V_{0.2}$	7.2356(1)	378.81(1)		
$YCo_{1.8}V_{0.2}H_{3.2}$	7.713(2)	458.84(2)	21.13	1.07

Under appropriate hydrogenation conditions these alloys absorb a large amount of hydrogen forming crystalline hydrides. The unit cell volume expansion is up to ~20%. Substitution of Co by V slightly decreases the hydrogen storage capacity of the alloys. XRD powder data of $YCo_{3-x}V_x$ ($x = 0$, 0.1 and 0.2) hydrides (see Fig. 1b, Table 1) confirmed that the structure of the parent compounds and their hydrides remains unchanged. The substitution of Co by V causes a slight decrease of the c/a ratio, but hydrogenation causes an opposite effect, c/a values increase proportionally with increasing hydrogen content in these alloys (see Table 1). This effect is well visible when comparing the XRD patterns of the parent and hydrogenated pseudo-binaries (see Fig. 1).

The solid solution $YCo_{2-x}V_x$ ($x = 0$, 0.1 and 0.2) belongs to the $MgCu_2$ structure type (space group $Fd\bar{3}m$). The cubic lattice parameter increases with growing V content (Table 3). The XRD pattern of $YCo_{1.8}V_{0.2}$ is shown in Fig. 2a, the corresponding refined final atomic parameters are presented in Table 4.

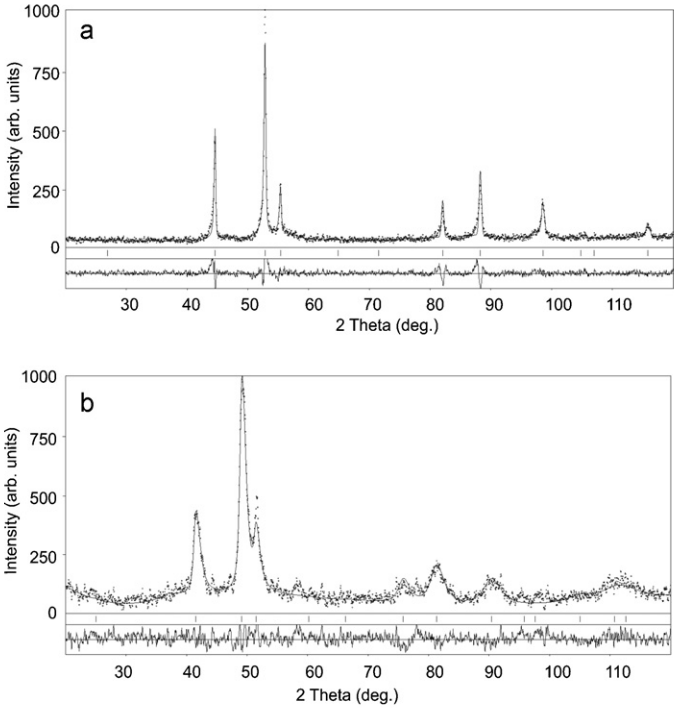

Fig. 2. Observed (points), calculated (line) and difference (bottom) X-ray diffraction patterns of $YCo_{1.8}V_{0.2}$ (a) and $YCo_{1.8}V_{0.2}H_{3.2}$ hydride in $MgCu_2$-type structure (b).

Hydrogen absorption of $YCo_{2-x}V_x$ ($x = 0$, 0.1 and 0.2) alloys was investigated with above mentioned smooth hydrogenation conditions. All samples absorb a large amount of hydrogen (~3.2–3.5 at.H/f.u.) and form crystalline hydrides (Fig. 2b) which preserve the structure of the parent compound. Hydrogenation causes pronounced lattice distortions which are visible when comparing XRD profiles of the parent alloy and its hydride (see Fig. 2a and b). For $YCo_{2-x}V_x$ ($0 < x \leq 0.2$) alloys hydrogen absorption capacity slightly decreases with increasing vanadium content in this solid solution (see Table 3).

3.1. Magnetic properties of YCo_2 based compounds and their hydrides

Shown in Fig. 3a is the magnetization at 0.1 T as a function of temperature for the parent $YCo_{2-x}V_x$ compounds in comparison with the corresponding β-phase hydrides. The substitution of Co by V induces weak ferromagnetism in the archetypical itinerant electron metamagnet YCo_2 with Curie temperatures of 175 K and 110 K and a mean 3d-moment of $0.14\mu_B$ and $0.07\mu_B$ at 6 T and 2.5 K for $x = 0.1$ and $x = 0.2$, respectively (see also Fig. 3b). Note, we use the notion mean 3d moment, rather than moment/Co-atom to be comparable with the moments given in the literature and because the hybridization of the V-3d states cannot be disentangled from those of the Co-3d states. Hydrogen absorption enhances this moment and causes a hysteric behaviour at low temperatures persisting up to 25 K being associated with coercitivities of about 0.1 T. The largest value of the hydrogen induced Co moment of about $0.2\mu_B$/Co is observed in $YCo_2H_{3.5}$ in good agreement with previous studies [21,22] where the metamagnetic features of YCo_2H_y and $Y(Co_{0.925}Al_{0.075})_2H_y$ were studied in pulsed fields up to 50 T. According to these reports the critical field of the metamagnetic transition is reduced in the α-phase ($y < 0.3$) and the α-phase hydrides remain itinerant electron metamagnets while weak ferromagnetism occurs in the β-phase hydrides ($1.5 > y > 3.5$). An analogous behaviour is also observed here (see Fig. 3). The ordering temperature of the induced moment caused by V substitution is reduced to below 30 K under hydrogenation and exhibits a comparably similar temperature dependence as that of the YCo_2H_y hydrides although the parent material is an itinerant electron metamagnet while the parent V substituted compounds are weak ferromagnets.

Note, a small ferromagnetic moment is observed in all β-hydrides in this solid solution but has been also detected for YCo_2H_y [21] persisting up to above room temperature. It is rather difficult to disentangle the intrinsic hydrogen induced Co-moment from a possible contribution due to structural disorder, which is obvi-

Table 4
Refined atomic parameters, site occupations (G) and isotropic temperature coefficients (B_{iso}) for $YCo_{1.8}V_{0.2}$ ($MgCu_2$-type structure, $R_I = 0.0415$).

Atom	Site	x/a	y/b	z/c	G	B_{iso} (Å^2)
Y	8*b*	3/8	3/8	3/8	1	0.39(3)
M	16*c*	0	0	0	0.90(1) Co + 0.10(1) V	0.47(3)

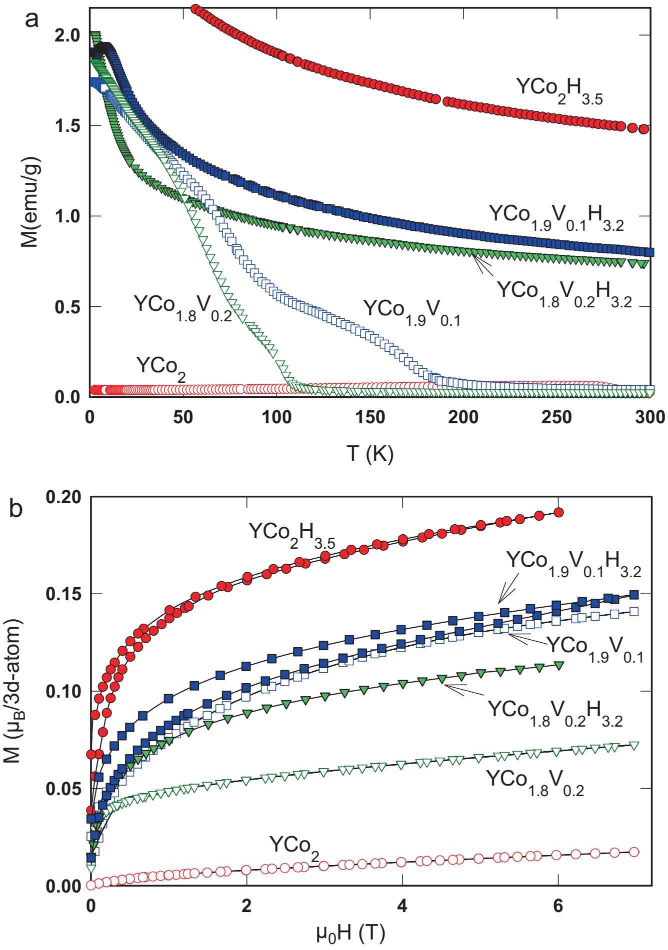

Fig. 3. Temperature dependent magnetization of $YCo_{2-x}V_x$ (open symbols) and the corresponding hydrides in the β-phase (full symbols) at 0.1 T (a); Magnetization as a function field for $YCo_{2-x}V_x$ (open symbols) and the corresponding hydrides in the β-phase (full symbols) at 2.5 K (b).

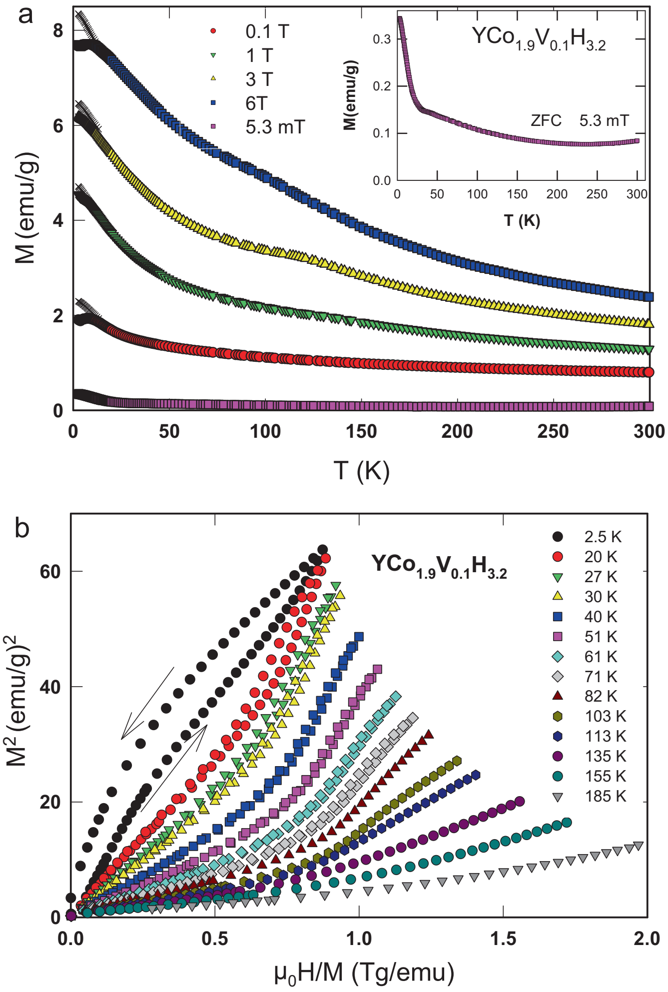

Fig. 4. Temperature dependent zero field cooled (ZFC) magnetization as a function of various fields as labeled (a), the corresponding field cooled (FC) magnetization is indicated by (×); inset in (a): ZFC magnetization at 5 mT. Magnetic isotherms plotted as M^2 versus H/M (Arrott plots) of $YCo_{1.9}V_{0.1}H_{3.2}$ (b).

ous from the significant line broadening in the X-ray pattern of the hydride (see Fig. 2). It is worthwhile to note that amorphous YCo_2 and amorphous $YCo_2H_{3.5}$ are ferromagnets; the latter with a moment of 1.1μ_B/Co and a T_c above 500 K [22] and also nanocrystalline YCo_2 (with a grain size of 20–30 nm) is ferromagnetic with a moment of 0.45μ_B/Co and a T_c of 563 K [31]. Furthermore a ferromagnetic surface of bulk paramagnetic YCo_2 was observed with photoelectron spectroscopy, in particular, Co atoms in the (1 1 1) surface layers of bulk paramagnetic YCo_2 are intrinsically ferromagnetic owing to an increase of the density of states at the Fermi level because of the reduced atomic coordination at the surface [32]. As all our hydrides are powder samples with a grain size of 5–30 μm yielding a significantly larger surface contribution than bulk specimens, the spontaneous moment of the hydrides persisting up to room temperature may to some extent arise from a grain size effect, structural disorder and/or surface contribution. A further question remains whether the shoulder of the magnetization of $YCo_{2-x}V_x$ at about 100 K and 80 K for $x = 0.1$ and $x = 0.2$, which is washed out in fields above 1 T, is an intrinsic property or arises from a secondary phase although neither in XRD nor in micrographs a secondary phase has been detected.

A detailed characterization of the temperature and field dependence of the magnetization of $YCo_{1.9}V_{0.1}H_{3.2}$ is displayed in Fig. 4a and b, respectively. The difference between field cooling (FC) and zero field cooling (ZFC) indicates a freezing of the induced moments at low temperatures which persists up to 6 T, and may thus be associated with structural disorder during hydrogenation. The low field magnetization shown in the inset of Fig. 4a reveals a rapid drop up to about 30 K which is tentatively attributed to the ordering temperature of the intrinsic hydrogen induced moment being washed out with raising fields. Even above 30 K the remaining magnetization is strongly field dependent and exhibits at low fields (5.3 mT) a broad maximum at about room temperature reminiscent of the susceptibility of YCo_2 (see inset in Fig. 4a) and may therefore be attributed to the magnetization arising from structural disorder observed in all YCo_2 based hydrides [21,22]. The magnetic isotherms, plotted as M^2 versus H/M (Arrott plots), presented in Fig. 4b clearly indicate up to room temperature a spontaneous magnetization (0.5 emu/g or 0.01μ_B/3d-atom) and a hysteresis at low temperatures which is almost diminished at 30 K but is still visible up to 70 K. The significant change of the slope of the Arrott plots at higher fields in the temperature window of 30–100 K can be interpreted as precursor of a metamagnetic transition at higher fields. On the other hand the high field slope of the Arrott plots extrapolates to finite H/M values and indicate paramagnetic behaviour of the intrinsic part of the magnetization while the low field part even up to room temperature extrapolates to finite M^2 values resulting in a spontaneous moment up to room temperature which thus may be attributed to a grain size and/or surface effects.

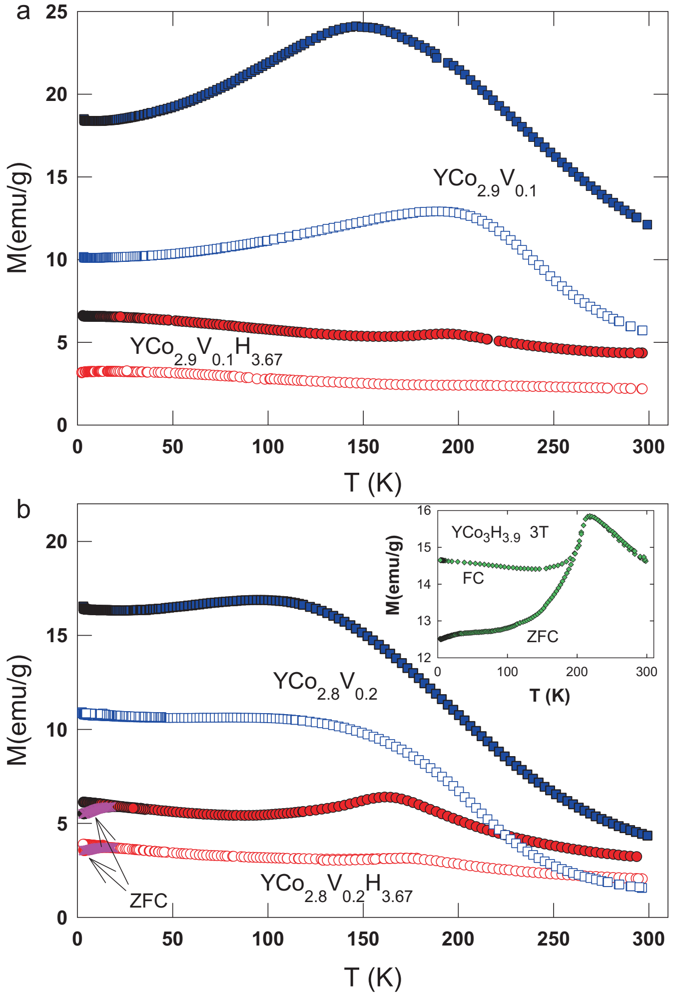

Fig. 5. Temperature dependence of the magnetization of $YCo_{2.9}V_{0.1}$ and $YCo_{2.9}V_{0.1}H_{3.67}$ (a) at 1 T (open symbols) and at 3 T (full symbols); Temperature dependence of the magnetization of $YCo_{2.8}V_{0.2}$ and $YCo_{2.8}V_{0.2}H_{3.75}$ (b) at 1 T (open symbols) and at 3 T in the FC state (full symbols) and ZFC state (×); inset: magnetization as a function of temperature for $YCo_3H_{3.9}$ at 3 T for zero field cooling (ZFC) and field cooling (FC).

To summarize the significant general features of the YCo_2 based compounds and hydrides: Substitution of Co by V induces weak ferromagnetism with rather sharp transition temperatures in YCo_2 being on the verge to the onset of magnetism. Hydrogen absorption enhances the mean 3d-moment at low temperatures whereby the saturation is by far not attained at low temperatures and 6 T. This enhancement is significantly larger in $YCo_2H_{3.5}$ than in the V substituted hydrides. In the latter the rather sharp transition temperature of the parent compounds is washed out and reduced to 30 K concomitant with the appearance of a small spontaneous magnetization persisting up to room temperature which, however, is due to structural distortions, grain size and/or surface effects rather than to be an intrinsic property of YCo_2 based β-phase hydrides.

3.2. *Magnetic properties of YCo_3 based compounds and their hydrides*

Ternary alloys $YCo_{3-x}V_x$ ($x = 0.1$ and 0.2) exhibit long range magnetic order and can by analogy with YCo_3 characterized as complex ferrimagnets. Shown in Fig. 5a and b are the temperature dependent magnetizations of $YCo_{3-x}V_x$ ($x = 0.1$ and 0.2) in comparison with their hydrides. The substitution of Co by V reduces T_c from 301 K in YCo_3 [6] to 255 K and 225 K for $x = 0.1$ and $x = 0.2$, respectively. The broad maximum of the magnetization of $YCo_{2.9}V_{0.1}$ (less distinct for $x = 0.2$) becomes more pronounced at higher fields and is shifted to lower temperatures with growing external fields. This can be attributed to a weakening of the ferrimagnetic interactions with rising external fields which thus causes the significant maximum of $M(T)$. According to the distinct temperature dependence of the magnetization this type of ferrimagnetism can be classified as P-type in terms of Néel's categorization of two sublattice ferrimagnets with a particular ratio of molecular field coefficients [33]. In this rather simple and phenomenological model the shape of the temperature dependence of the magnetization depends on the relative strengths of the molecular field coefficients γ_{aa} and γ_{bb} of the A and B sublattice, respectively, normalized with the intermolecular field coefficient between both sublattices γ_{ab} (i.e. $\alpha = \gamma_{aa}/\gamma_{ab}$, $\beta = \gamma_{bb}/\gamma_{ab}$; where the A sublattice is that with the larger magnetization). A conventional Brillouin-like temperature dependence of the magnetization, referred to as Q-type, is obtained if α and β is of comparable magnitude. A transition occurs from the Q-type to a P-type temperature dependence, characterized by a more or less pronounced maximum of the magnetization, when β becomes dominant, whereas the dominance of α yields a compensation point in the magnetization being referred to as a N-type magnetization.

Thus, the ferrimagnetic Q-type feature of YCo_3 is converted to a P-type due to substitution of Co by V in the pseudobinaries which tentatively can be interpreted by an attenuation of the exchange interactions of that sublattice with the larger magnetization as well the intersublattice interactions leading both to a reduction of T_c and the mean 3d-moment.

Hydrogenation reduces the 3d-moment (see Fig. 5c) at low temperatures as well as the ordering temperature if we associate the weak maximum at 200 K and 180 K in the corresponding γ-hydrides ($x = 0.1$ and $x = 0.2$) with the intrinsic antiferromagnetic order. This maximum in the hydrides is also strongly field dependent and is shifted to lower temperatures with rising external fields, but appears to be superimposed on a ferromagnetic background persisting up to above room temperature.

A comparison of the V-substituted γ-hydrides with $YCo_3H_{3.9}$ – where the complex antiferromagnetic structure has been resolved with neutron diffraction [16] – shows that the peak of $M(T)$ associated with the onset of antiferromagnetic order is also superimposed upon an even larger magnetic background with a mean Co moment of about $0.1\mu_B$ than the hydrides of the solid solution, see inset of Fig. 5b. The amount of this background in $YCo_3H_{3.9}$ depends largely upon field cooling or zero field cooling and can be attributed to domain wall pinning since the magnetic isotherm of $YCo_3H_{3.9}$ exhibits at about 2 T a first metamagnetic transition associated with a distinct hysteresis displayed in the inset of Fig. 6. The main metamagnetic transition occurs at about 17 T (which is far beyond the field limit of the SQUID) and was observed in a single crystal along the *c*-axis by Bartashevich et al. [6] where also a magnetic background was detected. Therefore, this magnetic background is presumably due to Co precipitates rather than due to grain size or surface effects although the crystal structure contains YCo_2 and YCo_5 building blocks. Furthermore, the line broadening of the hydrided powder specimens is negligible in particular with respect to the Laves phase hydrides. The difference between FC and ZFC is rather small for the V-substituted compounds being resolvable in the given scale for $YCo_{2.8}V_{0.2}H_{3.75}$ only and can be attributed to the hysteresis apparent in the corresponding isotherms at 2.5 K in Fig. 6. Finally, we derive from Fig. 6 the general trend of the YCo_3 based compounds that the mean 3d-moment of the anisotropic ferrimagnet YCo_3 ($0.5\mu_B$/Co [6]) is significantly reduced by V-substitution as well as in the corresponding antiferromagnetic γ hydrides at low temperatures.

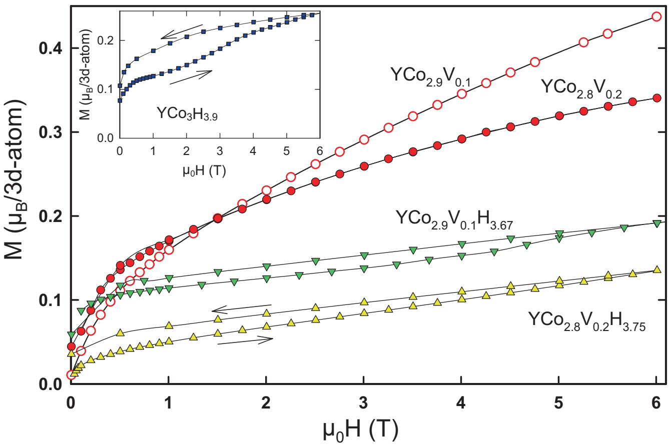

Fig. 6. Magnetization as a function field for $YCo_{3-x}V_x$ and the corresponding γ-phase hydrides at 2.5 K; inset: isothermal magnetization of $YCo_3H_{3.9}$.

4. Conclusions

The pseudo-binary compounds $YCo_{2-x}V_x$ and $YCo_{3-x}V_x$ ($x = 0.1$ and 0.2) preserve their crystal structure under a moderate hydrogen absorption process at room temperature yielding the corresponding hydrides in the β- and γ-phase, respectively, as powder specimens. The XRD-line broadening of the hydrided powder specimens is pronounced in the former but negligible in the latter.

The general features of YCo_2 and YCo_3 based compounds and their hydrides are significantly different although the structure of YCo_3 contains YCo_5 as well as YCo_2 building blocks. In YCo_2 the prime example for an itinerant electron metamagnet substitution of Co by V induces weak ferromagnetism with rather sharp transition temperatures below 175 K. Hydrogenation distinctively broadens and reduces T_c in the solid solution but enhances the 3d-moment at low temperatures whereby a small spontaneous moment is preserved up to above room temperature being due to structural distortions and/or surface effects rather than to be an intrinsic property of these hydrides.

The ferrimagnetic behaviour of YCo_3 becomes more pronounced by substitution of Co by V going hand in hand with a reduction of T_c from 301 K to 225 K for $x = 0.2$. Thus V substitution causes a transition from a Q-type to a P-type temperature dependence of the magnetization in terms of Néel's classification of ferrimagnetic coupling being due to a weakening of both the exchange interaction of the sublattice with the larger magnetization as well the intersublattice exchange. Ferrimagnetism of the parent compounds is converted into antiferromagnetism under hydrogenation which is superimposed on a ferromagnetic background persisting up to above room temperature. This soft ferromagnetic background might be attributed to Co precipitates, rather than to structural distortions and/or surface effects which on the other hand is obviously the origin of the small ferromagnetic background in all Laves phase hydrides $YCo_{2-x}V_xH_y$ but appears to be not an intrinsic property of both systems.

Acknowledgment

This work was supported by the Ukrainian Austrian WTZ project No. UA 06/2009.

References

[1] K. Yvon, P. Fischer, Hydrogen in Intermetallic Compounds I. Electronic, Thermodynamic and Crystallographic Properties, Preparation, vol. 63, Springer-Verlag, Berlin, 1988, pp. 87–138.

[2] G. Wiesinger, G. Hilscher, in: K.-H.-J. Buschow (Ed.), Handbook on Magnetic Materials, vol. 17, Elsevier B.V., 2008, pp. 293–456 (Chapter 5).

[3] D.T. Cromer, C.E. Olsen, Acta Crystallogr. 12 (1959) 689.

[4] B.D. Dunlap, P.J. Viccaro, G.K. Shenoy, J. Less-Common Met. 74 (1980) 75.

[5] X.Y. Cui, J. Liu, P.A. Georgiev, I. Morrison, D.K. Ross, M.A. Roberts, K.A. Anderson, M. Telling, D. Fort, Phys. Rev. B 76 (2007) 184443.

[6] M.I. Bartashevich, T. Goto, M. Yamaguchi, I. Yamamoto, A.V. Andreev, Solid State Commun. 82 (1992) 201.

[7] M. Yamaguchi, I. Yamamoto, M.I. Bartashevich, H.A. Katori, T. Goto, J. Alloys Compd. 231 (1995) 159.

[8] M. Latroche, A. Percheron-Guégan, J. Alloys Compd. 356–357 (2003) 461.

[9] R.H. Van Essen, K.H.J. Buschow, J. Less-Common Met. 70 (1980) 189.

[10] M.J. Benham, S. Bennington, D.K. Ross, D. Noreus, M. Yamaguchi, Z. Phys. Chem. Neue Folge 163 (1989) 283.

[11] M.I. Bartashevich, H.A. Katori, T. Goto, I. Yamamoto, M. Yamaguchi, Physica B 201 (1994) 135.

[12] J. Liu, D.P. Broom, P.A.L. Georgiev, D.K. Ross, J. Alloys Compd. 356–357 (2003) 174.

[13] M.I. Bartashevich, A.N. Pirogov, V.I. Voronin, T. Goto, M. Yamaguchi, I. Yamamoto, J. Alloys Compd. 231 (1995) 104.

[14] M.I. Bartashevich, T. Goto, M. Yamaguchi, I. Yamamoto, Physica B: Cond. Matter 294–295 (2001) 186.

[15] M. Yamaguchi, I. Yamamoto, T. Goto, Z. Phys. Chem. Neue Folge 163 (1989) 677.

[16] J. Liu, X.-Y. Cui, P.A. Georgiev, I. Morrison, D.K. Ross, M.A. Roberts, K.A. Anderson, M. Telling, D. Fort, Phys. Rev. B 76 (2007) 184444.

[17] V.A. Yartys', I.I. Bulyk, O.M. Sichevich, N.I. Tomaszczuk, J. Alloys Compd. 189 (1992) L27.

[18] E. Gratz, A.S. Markosyan, J. Phys. Cond. Matter 13 (2001) R385.

[19] E. Burzo, A. Chełkowski, H.R. Kirchmayr, in: H.P.J. Wijn (Ed.), Landolt-Börstein, Numerical Data and Functional Relationship in Science and Technology, New Series, Magnetic Properties of Metal, vol. 19-D2, Springer, Berlin, 1990.

[20] T. Goto, K. Fukamichi, T. Sakakibara, H. Komatsu, Solid State Commun. 72 (1989) 889.

[21] K. Ishikawa, M. Yamaguchi, I. Yamamoto, S. Mizusaki, F. Ishikawa, T. Goto, J. Alloys Compd. 356–357 (2003) 227.

[22] N.V. Mushnikov, T. Goto, V.S. Gaviko, N.K. Zajkov, A.V. Ilyushenko, J. Alloys Compd. 278 (1998) 44.

[23] N.V. Mushnikov, V.S. Gaviko, T. Goto, J. Alloys Compd. 398 (2005) 36.

[24] N.V. Mushnikov, V.S. Gaviko, A.V. Korolyov, N.K. Zajkov, J. Alloys Compd. 218 (1995) 165.

[25] F. Pourarian, W.E. Wallace, S.K. Malik, J. Magn. Magn. Mater. 25 (1982) 299.

[26] Y. Öner, O. Kamer, J. Alloys Compd. 464 (2008) 51.

[27] H. Michor, B. Kotur, O. Myakush, G. Hilscher, J. Phys.: Conf. Ser., in press.

[28] R.A. Young, The Rietveld Method, Oxford University Press, 1993.

[29] J. Rodrigues-Carvajal, Program: FullProf. Lab. Leon Brillouin, CEA-CNRS, 1998.

[30] L.G.P. Akselrud, Yu. Zavalii, Yu.N. Grin, V.K. Pecharsky, B. Baumgartner, E. Wolfel, Mater. Sci. Forum 133–136 (1993) 335.

[31] S.N. Jammalamadaka, E.V. Sampathkumaran, V.S.N. Murthy, G. Markandeyulu, Appl. Phys. Lett. 92 (2008) 192506.

[32] S.Yu. Dedkov, C. Laubschat, S. Khmelevsky, J. Redinger, P. Mohn, M. Weinert, J. Phys. Conf. Ser. 100 (2008) 07028.

[33] J.S. Smart, Effective Field Theories of Magnetism, Saunders, Philadelphia & London, 1966.